Moment analysis of near-equilibrium binding interactions during electrophoresis

Yousef Daneshbod
Department of Mathematics, Claremont Graduate University, Claremont, California 91711, USA

James D. Sterling and Ali Nadim*
Keck Graduate Institute, Claremont, California 91711, USA

(Received 15 February 2006; revised manuscript received 14 August 2007; published 30 November 2007)

The electrophoretic transport of three chemically reacting species, two of which can bind reversibly to form the third, is analyzed mathematically. The species are assumed to move horizontally through a long channel with different electrophoretic mobilities and diffusion coefficients. By considering small perturbations of the system about equilibrium or when one of the two binding species is much more abundant than the other, the governing advection-reaction-diffusion equations can be linearized and studied via the method of moments. The result is a set of coupled ordinary differential equations for the moments that can be solved analytically. Analysis of the long-time evolution of the moments yields mean velocities and dispersion coefficients for each species. The results provide a method for measuring the rate and equilibrium constants of binding reactions using capillary electrophoresis.

DOI: 10.1103/PhysRevE.76.051922 PACS number(s): 82.45.−h, 82.40.Ck, 87.15.Tt

I. INTRODUCTION

Binding reactions and biomolecular recognition events are central to many biological and pharmaceutical processes, including enzyme-substrate, antibody-antigen, drug-protein, protein-DNA, and ligand-receptor interactions. For instance, quantifying protein-protein binding interactions have a significant impact on increasing the throughput for drug design [1]. In addition, capillary electrophoresis (CE) microfluidic systems that consume low quantities of reagents, integrate multiple assay steps, and use computer control to govern the reaction conditions have undergone significant development in recent years [2]. Therefore, devising techniques based on CE for quantifying binding interactions would be timely.

A typical reversible binding process can be represented via

$$A + B \underset{k_{\text{off}}}{\overset{k_{\text{on}}}{\rightleftharpoons}} C, \tag{1}$$

in which molecules A and B bind to form the complex C. The rate constants for the forward (association) and reverse (dissociation) reactions are denoted by k_{on} and k_{off}, respectively. At equilibrium, the rates of forward and reverse reactions, given by the law of mass action, balance each other to yield

$$k_{\text{on}}[A]_{\text{eq}}[B]_{\text{eq}} = k_{\text{off}}[C]_{\text{eq}} \Rightarrow K_D \equiv \frac{k_{\text{off}}}{k_{\text{on}}} = \frac{[A]_{\text{eq}}[B]_{\text{eq}}}{[C]_{\text{eq}}}. \tag{2}$$

Binding reactions can therefore be characterized via the two rate constants k_{on} and k_{off}. The equilibrium dissociation constant K_D (or its reciprocal, the affinity or binding constant) is given by the ratio of the rate constants.

One method for measuring the real time kinetics of binding and dissociation reactions is based on surface plasmon resonance (SPR), which is a recently developed spectroscopic method based on sensing refractive index changes near the surface of a metal film [3]. Conventional SPR is applied in specialized biosensing instruments. However, these instruments use expensive sensor chips with limited reuse potential and require complex chemistry for ligand or protein immobilization [4].

Our goal in the present theoretical contribution is to suggest a technique, based on results from detailed analysis of a mathematical model, for measuring the rate and equilibrium constants via capillary electrophoresis. Capillary electrophoresis has already established itself as a powerful tool for the analysis of a variety of analytes, including chiral molecules, proteins, carbohydrates, and DNA [5,6]. This technique, in its most basic terms, separates charged molecules on the basis of differences in the velocities at which they migrate in an electric field. As will be argued here, for the case of reversible binding reactions where the mobilities of the molecular species are different, by monitoring the electropherogram in certain CE experiments, it should be possible to infer the associated rate constants.

This is similar in spirit to so-called affinity capillary electrophoresis (ACE), which is a technique for measuring equilibrium binding constants [7–11]. The majority of applications of ACE, however, determine only the equilibrium constant K_D and not the rate constants themselves. In ACE, the capillary is typically filled with a buffer containing either the ligand or the analyte and a sample containing the other molecule is injected and passed through the capillary by electrophoresis. The equilibrium constant is then determined by measuring the changes in the mobilities of the injected sample or by analyzing the peak areas or plateau heights in the electropherogram [8]. Other CE-related methods for measuring equilibrium binding constants, including the Hummel-Dreyer (HD), vacancy ACE (VACE), vacancy peak (VP), and frontal analysis [12] (FA) methods, are reviewed in Ref. [8].

A more recent development in this area is the so-called nonequilibrium capillary electrophoresis of equilibrium mixtures (NECEEM), developed by Berezovski and Krylov [13,14], which has the potential for yielding both the equi-

*Also at Department of Mathematics, Claremont Graduate University, Claremont, CA 91711. nadim@kgi.edu

librium and the kinetic parameters simultaneously. Recently this method has been used for selection of aptamers which are ligands selected from large libraries of random DNA sequences and capable of binding different classes of targets with high affinity and selectivity [15]. This method has a number of advantages over conventional approaches. First, NECEEM-based selection has exceptionally high efficiency, which allows aptamer development with fewer rounds of selection. Second, NECEEM can be used both for selecting aptamers and finding their binding parameters.

Okhonin *et al.* [16] have developed a mathematical model of NECEEM, describing the concentration of components involved in complex formation as a function of time. This model is used for finding binding parameters of complex formation by nonlinear regression of NECEEM electropherogram obtained experimentally. The model considers the simplified limit where the association reaction can be neglected (i.e., when the electrophoretic zones of the two binding species are well separated) so that the governing partial differential equations become linear. Having such an analytical solution is found to be helpful, enabling linear regression to be performed on the electropherograms to obtain k_{off} and K_D.

The theoretical analysis in the present contribution can also be classified as pertaining to nonequilibrium CE since it is based on a nonequilibrium dynamic separation of the mixture of species involved in a binding reaction, within a CE system. Our theoretical approach differs from those of Refs. [13–16], as well as from the more standard affinity CE analyses, in that we suggest two limiting cases in which the nonlinear coupled system governing the process can be linearized and solved analytically using the method of moments. As such, analytical expressions are derived for the evolution of the moments that can be extracted from corresponding electropherograms. Our analysis also suggests the possibility of extracting the rate constants (and not just the equilibrium binding constant) from the more standard ACE system.

We begin with the full partial differential equations governing the transport of the reacting species but analyze them in two linearized limits based on the method of moments, similar to that used in classical Taylor dispersion theory [17,18] for transport of nonreacting species in pressure-driven laminar flows. For purely diffusive scalar dispersion processes, Taylor's intuitive method [17] for constructing dispersion coefficients was formalized by Aris [18] who introduced the method of moments. This framework was subsequently greatly generalized by Brenner who introduced so-called generalized Taylor dispersion theory [19,20] or the theory of macrotransport processes [21]. Berne and Giniger [22] have proposed a theoretical model based on electrophoretic light scattering for determining rate constants in dimerization reaction of globular proteins. Their method in principle is analogous to the study of exchange rates in NMR. For systems which exchange matter with their surroundings or in which a chemical reaction takes place along the lateral boundaries, Degance and Johns [23] have given a dispersion approximation to the vector convective diffusion equations. They have also extended their results to the dispersion of chemically active solutes under the action of a rectilinear flow field confined by a cylindrical surface which catalyzes a first-order chemical rearrangement of the solute constituents [24]. Some of the applications of Taylor-Aris dispersion theory include the work of Bello *et al.* [25] who successfully applied the moment theory to measure diffusivities of various molecules quickly and inexpensively to within 1% or 2% of published values, that of Stellwagen *et al.* [26] who made similar measurements of diffusivities of small DNA molecules by CE, and that of Dorfman and Brenner [27] who used graph-theoretical techniques, combined with generalized Taylor-Aris dispersion theory, to model microfluidic chromatographic separation devices. Dorfman and Brenner [28] have also used a method-of-moment scheme similar in spirit to the present method for computing the long-time mean velocity and dispertivity of a two-state particle undergoing one-dimensional convective-diffusive motion accompanied by a reversible linear transition between these states. They have shown that in the absence of molecular diffusion, the average transport of the "composite" particle exhibits gaussian diffusive behavior in the long-time limit due to the stochastic nature of the transport phenomena induced by the interstate transition. The moment method and Taylor dispersion concepts have also been applied by Ghosal and Horek [29] to model gradient focusing of trace analytes.

Other methods include the so-called center–invariant-manifold theory, originating from early pioneering works of Poincaré [30], Lyapunov [31], and Hadamard [32] and later extended by Pliss [33], Kelley [34], and others to include finite-dimensional dynamical systems. Balakotaiah and Chang [35] have used this theory to investigate the effective dispersion of a chemically active solute in unidirectional laminar flow in a channel of constant cross-sectional area. They have shown that in slow bulk reactions a steady-state dispersion due to the coupling of reaction and transverse velocity gradient can arise.

In the following, we consider the electrophoretic transport of three chemically reacting species (two of which can bind reversibly to form the third) moving horizontally through a long channel with their respective mobilities and diffusivities. By linearizing the system about its equilibrium state or when one of the two binding species is much more abundant than the other, a set of coupled ordinary differential equations are derived which describe the moments of the linearized convection-reaction-diffusion equations. Analytical results are obtained for the long-time evolution of the moments, yielding mean velocities and dispersivities for the relevant molecules. The results suggest a method for measuring the rate and equilibrium constants of binding reactions using capillary electrophoresis.

II. MATHEMATICAL MODEL

Consider a system composed of three chemically reacting species, referred to as C_1, C_2, and C_3, moving along an infinite channel and undergoing the following reversible reaction

$$C_1 + C_2 \underset{k_{\text{off}}}{\overset{k_{\text{on}}}{\rightleftharpoons}} C_3, \tag{3}$$

where k_{on} and k_{off} are the forward (association) and reverse (dissociation) rate constants. Since the species are migrating,

diffusing, and reacting within a long one-dimensional channel, the governing equation describing the change in concentrations of the three species as a function of space and time, $c_i(x,t)$ $(i=1,2,3)$, is given by

$$\frac{\partial \vec{c}}{\partial t} + U\frac{\partial \vec{c}}{\partial x} = D\frac{\partial^2 \vec{c}}{\partial x^2} + \vec{h}(\vec{c}, k_{\text{on}}, k_{\text{off}}), \tag{4}$$

where $\vec{c}$ is the concentration vector defined as

$$\vec{c} = \begin{bmatrix} c_1 \\ c_2 \\ c_3 \end{bmatrix} \tag{5}$$

and U and D are the velocity and the diffusivity matrices, given, respectively, by

$$U = \begin{bmatrix} u_1 & 0 & 0 \\ 0 & u_2 & 0 \\ 0 & 0 & u_3 \end{bmatrix}, \quad D = \begin{bmatrix} D_1 & 0 & 0 \\ 0 & D_2 & 0 \\ 0 & 0 & D_3 \end{bmatrix}. \tag{6}$$

The scalar quantities $c_i(x,t)$, u_i, and $D_i(i=1,2,3)$ describe the concentration field, and electrophoretic velocity, and molecular diffusivity of the ith species, respectively. The velocities during CE are themselves typically given by $u_i=\mu_i E$ in which μ_i is the electrophoretic mobility of the molecule and E is the strength of the electric field along the channel. $\vec{h}$ is the nonlinear second-order reaction rate vector given by

$$\vec{h} = \begin{bmatrix} -k_{\text{on}}c_1c_2 + k_{\text{off}}c_3 \\ -k_{\text{on}}c_1c_2 + k_{\text{off}}c_3 \\ +k_{\text{on}}c_1c_2 - k_{\text{off}}c_3 \end{bmatrix}. \tag{7}$$

We also assume the following set of boundary conditions for Eq. (4):

$$\lim_{|x|\to\infty} |x|^m \vec{c}(x,t) = \vec{0} \quad (m = 0,1,2,\ldots), \tag{8}$$

i.e., faster-than-algebraic decay of the concentration fields at infinity, along with an arbitrary, integrable set of initial conditions.

Two linearized limits

There are two major obstacles in finding an analytical solution to Eq. (4). First, the system is coupled via the reaction term $\vec{h}$ and, second, the system is nonlinear. There are, however, two special limits for which the governing equations can be linearized into forms that are amenable to analytical treatment.

One interesting and important case is when the concentration of one of the two binding species—say, that of species 2—is much larger than the other, causing reaction (3) to simplify to the binary form

$$C_1 \underset{k_2}{\overset{k_1}{\rightleftharpoons}} C_3, \tag{9}$$

where

$$k_1 = k_{\text{on}}c_{o2}, \quad k_2 = k_{\text{off}}, \tag{10}$$

and c_{o2} denotes the initial concentration of species 2, which remains nearly constant throughout the process. This limit can be experimentally realized, for instance, by filling the entire channel with a solution of species C_2 at a uniform concentration; then locally injecting a small solution of C_1 into the channel at a concentration that is lower than that of C_2, and, finally, applying the electric field that gives rise to electrokinetic transport of the species within the channel and monitoring the concentration profiles of C_1 and the bound complex C_3 in the channel as is commonly done during electrophoresis. In this limit, one only needs to keep track of the concentrations $c_1(x,t)$ and $c_3(x,t)$ and Eq. (4) simplifies to

$$\frac{\partial \vec{c}}{\partial t} + U\frac{\partial \vec{c}}{\partial x} = D\frac{\partial^2 \vec{c}}{\partial x^2} + K\vec{c}, \tag{11}$$

where it should be understood that $\vec{c}=[c_1\ c_3]^T$ is now a 2-vector and matrices U and D are 2×2 diagonal matrices that contain the velocities and diffusivities of species 1 and 3. In Eq. (11), the reaction rate matrix K is given by

$$K = \begin{bmatrix} -k_1 & k_2 \\ k_1 & -k_2 \end{bmatrix}. \tag{12}$$

A second more complex limit in which Eq. (4) can be linearized is by considering small perturbations of the system around the three-species equilibrium state described by

$$c_i = c_i^e + \tilde{c}_i(x,t) \quad (i = 1,2,3), \tag{13}$$

where c_i^e and $\tilde{c}_i$ are the equilibrium and perturbed concentrations of species i, respectively. The equilibrium concentrations are assumed to be uniform in space and constant in time while the perturbations depend on space and time. Experimentally, this is equivalent to filling the channel with an equilibrium mixture first, then creating a small localized perturbation somewhere by modifying one or more of the concentrations (e.g., by local injection) and considering the evolution of the perturbations in space and time. When the means of detection is laser-induced fluorescence, one can further attach the fluorescent label to the injected species only, making the remaining background "transparent" to the detector. Substituting (13) into (4) and noting that

$$k_{\text{on}}c_1^e c_2^e = k_{\text{off}}c_3^e$$

results in the linearized system

$$\frac{\partial \tilde{\vec{c}}}{\partial t} + U\frac{\partial \tilde{\vec{c}}}{\partial x} = D\frac{\partial^2 \tilde{\vec{c}}}{\partial x^2} + K\tilde{\vec{c}}, \tag{14}$$

in which the matrix of reaction constants K has the form

$$K = \begin{bmatrix} -k_1 & -k_2 & k_3 \\ -k_1 & -k_2 & k_3 \\ k_1 & k_2 & -k_3 \end{bmatrix}, \tag{15}$$

where we have defined

$$k_1 = k_{\text{on}}c_2^e, \quad k_2 = k_{\text{on}}c_1^e, \quad k_3 = k_{\text{off}}. \tag{16}$$

III. MOMENT ANALYSIS

The above linear systems can be analyzed via the method-of-moments. In this method, we multiply the governing advection-diffusion-reaction equation (11) or (14) by x^m with $m=0,1,2,\ldots$, integrate over all x, and apply integration-by-parts as needed to obtain a corresponding set of ordinary differential equations for the moments. Typically, only the first three moments are needed to quantify the mean velocity and mean dispersivity of the species being transported. These are the zeroth, first, and second moments of the concentration vector, here denoted by $\vec{z}(t)$, $\vec{f}(t)$, and $\vec{s}(t)$, and, respectively, defined as

$$\vec{z}(t) = \int_{-\infty}^{\infty} \vec{c}\,dx, \tag{17}$$

$$\vec{f}(t) = \int_{-\infty}^{\infty} x\vec{c}\,dx, \tag{18}$$

$$\vec{s}(t) = \int_{-\infty}^{\infty} x^2\vec{c}\,dx. \tag{19}$$

[For the case of the ternary system (14), the moments are defined using the perturbation concentrations $\tilde{c}$ rather than $\vec{c}$.] Note that the zeroth moment describes the total amounts of the various species (or their perturbations) throughout the channel at any given time. The first moment, when normalized by the zeroth moment component by component, describes the location of the centroids of the perturbed concentration fields, and the second moment is related to the spread of the perturbed concentration about the centroid as usual.

Once the moments are computed, one can determine the effective long-time velocities and dispersivities of each of the species using the standard definitions [21]:

$$u_i^* = \lim_{t\to\infty} \frac{d}{dt}\left(\frac{f_i}{z_i}\right) \quad (i=1,2,3), \tag{20}$$

$$D_i^* = \lim_{t\to\infty} \frac{1}{2}\frac{d}{dt}\left[\left(\frac{s_i}{z_i}\right) - \left(\frac{f_i}{z_i}\right)^2\right] \quad (i=1,2,3). \tag{21}$$

In other words, the mean transport velocity is the long-time limit of the rate of change of the position of the centroid of the corresponding distribution for each of the species and the mean dispersion coefficient is one-half the slope of the linear increase in time of the mean-square displacement about the centroid, similar to any diffusive process.

A. Binary reaction

For simplicity in notation, the binary case is best described by renaming C_3 to C_2 temporarily and referring to the velocity and diffusivity of the complex by u_2 and D_2 as well. In other words, imagine the binary reversible system to correspond to

$$C_1 \underset{k_2}{\overset{k_1}{\rightleftharpoons}} C_2 \tag{22}$$

rather than the form given earlier. In particular, while we derived this system as a limiting case of the more general ternary binding reaction when one of the two species was more abundant than the other, it can also be thought of independently as describing any reversible binary reaction. For instance, C_1 and C_2 can refer to two different configurations or charged states of the same molecule that have different electrophoretic mobilities. In that case, one need not even consider the channel to have been filled by one of the binding species in advance and the analysis is more generally applicable.

Taking the first three spatial moments of Eq. (11), we obtain the following systems of ordinary differential equations:

$$d\vec{z}/dt = K\vec{z}, \tag{23}$$

$$d\vec{f}/dt = K\vec{f} + U\vec{z}, \tag{24}$$

$$d\vec{s}/dt = K\vec{s} + 2U\vec{f} + 2D\vec{z}, \tag{25}$$

where K is given by Eq. (12) and U and D are 2×2 counterparts of matrices given in Eq. (6). In order to find the mean velocities and dispersivities by means of formulas (20) and (21), we first need to obtain the longtime solution to Eqs. (23)–(25). This can be done in a straightforward manner with the help of the general solution presented in Appendix A. In the interest of brevity, in the following, we mainly provide the pertinent final solutions of the equations. The reader who wishes to follow the derivations more closely should review the appendix first.

From the initial conditions on the concentration fields, the initial values of the zeroth moments can be obtained. Call these z_{o1} and z_{o2} and the corresponding initial condition vector on the zeroth moment $\vec{z}_o=[z_{o1}\ z_{o2}]^T$. The long-time solution of Eq. (23) for the zeroth moments is found to tend to the constant

$$\vec{z} = \frac{z_{o1}+z_{o2}}{k_1+k_2}\begin{bmatrix} k_2 \\ k_1 \end{bmatrix} = M\vec{z}_o, \tag{26}$$

where matrix M is given by

$$M = \frac{1}{k_1+k_2}\begin{bmatrix} k_2 & k_2 \\ k_1 & k_1 \end{bmatrix}. \tag{27}$$

The ratio $z1/z2$ of the two components of the long-time zeroth moment vector is given by k_2/k_1 which corresponds to the equilibrium state of the binary reaction itself in the absence of spatial variations or temporal dynamics. This makes sense intuitively.

The first moment vector $\vec{f}(t)$ can be obtained by solving Eq. (24) and is found to be a linearly increasing function of time for long times. At this point we can determine the effective velocity of each species using definition (20). Interestingly, the mean velocities of the two species turn out to be the same and are given by

$$u_1^* = u_2^* = \frac{k_1u_2 + k_2u_1}{k_1+k_2} = \frac{u_1/k_1 + u_2/k_2}{1/k_1 + 1/k_2}, \tag{28}$$

which is in agreement with the result previously derived by Dorfman and Brenner [28].

TABLE I. Matrix form for the various long-time moments.

Moments[a]	Symbol	Matrix form
Zeroth	$\vec{z}$	$M\vec{z}_o$
First	$\vec{f}$	$MUM\vec{z}_o t - KUM\vec{z}_o/\lambda_1^2 + M\vec{f}_o$
Time derivative of second	$\frac{d}{dt}\vec{s}$	$2MUMUM\vec{z}_o t - 2MUKUM\vec{z}_o/\lambda_1^2 - 2KUMUM\vec{z}_o/\lambda_1^2$ $+2MUM\vec{f}_o + 2MDM\vec{z}_o$

[a]Long-time asymptotic form of the moments.

In other words, the centroids of both concentration fields tend to migrate along the channel at the same speed which is a weighted average of the individual velocities of the two species, weighted by the forward and reverse reaction time scales k_1^{-1} and k_2^{-1}.

While the two centroids do travel at the same mean speed, it turns out they are not actually coincident. Instead, the species with the higher mobility (higher advection velocity) is on average ahead of the slower species. The distance between the two centroids is a constant at long times, which can be calculated by subtracting the smaller of the two centroid positions, f_1/z_1 and f_2/z_2, from the other. Assuming that the centroids are roughly located at the peaks of their respective distribution, this "peak-to-peak" distance between the two distributions turns out to be

$$l = \frac{|u_2 - u_1|}{k_1 + k_2}. \tag{29}$$

That is, at long times, the two species concentration curves can approximately be described as partially overlapping traveling "pulses" that migrate down the channel at the same average speed, but with peaks that are displaced from one another by a constant value. These pulses do not maintain their width but also spread at a rate governed by the dispersivity.

To obtain this effective dispersion coefficient using the definition (21), we need to compute the time rate of change of the second moment by solving Eq. (25). The long-time evolution for the various moments are summarized in Table I (see Appendix A for a detailed derivation). In that table, M, U, K, and D are all 2×2 matrices given earlier, $\vec{f}_o$ is the vector of initial first moments, and $\lambda_1 = -(k_1 + k_2)$. Using Table I and the standard definition (21) the two dispersivities can be calculated as follows:

$$D_1^* = D_2^* = \frac{k_1 k_2}{k_1 + k_2}\left[\left(\frac{u_2 - u_1}{k_1 + k_2}\right)^2 + \frac{D_1}{k_1} + \frac{D_2}{k_2}\right], \tag{30}$$

also in agreement with the result in Ref. [28]. The dispersion coefficients include a weighted average of the individual molecular diffusivities D_1 and D_2, in addition to a contribution resulting from a combination of advection at different speeds and the reaction rates. This is similar in spirit to the so-called Taylor-Aris dispersion that occurs during Poiseuille flow in a tube in which, in addition to the molecular diffusivity, there is a Taylor contribution to the axial dispersion resulting from the nonuniformity of the flow within the tube cross section. In our model, although the axial transport is described by uniform velocities (plug flow) as typical of electrokinetic transport, the difference between the velocities of the two species in the reversible binary reaction gives rise to a similar extra contribution to the mean dispersivity.

B. Ternary reaction

For the ternary system governed by Eq. (14), a moment-based approach identical to the above yields a system of ordinary differential equations for the first three moments that are identical to Eqs. (23)–(25), but with the rate constant matrix K now given by Eq. (15) and the 3×3 velocity and diffusivity matrices given by Eqs. (6).

Beginning with an initial condition $\vec{z}_o$ on the zeroth moment (obtained simply by taking the zeroth moment of the given initial perturbation concentrations), the long-time solution of the zeroth moment is again found to be

$$\vec{z} = M\vec{z}_o, \tag{31}$$

where matrix M is now given by

$$M = \frac{1}{k_1 + k_2 + k_3}\begin{bmatrix} k_2 + k_3 & -k_2 & k_3 \\ -k_1 & k_1 + k_3 & k_3 \\ k_1 & k_2 & k_1 + k_2 \end{bmatrix}. \tag{32}$$

Note that the zeroth moment tends to a constant in time, determined solely by the rate constants and the initial condition. It can also be seen that unlike the binary case, positive perturbations of the concentrations might end up becoming negative in the long run. The corresponding long-time limits of the rate of change of the first- and second-moment vectors can also be obtained via Table I, where in this case $\lambda_1 = -(k_1 + k_2 + k_3)$. Therefore, as with the binary case, if we divide each component of the first- and second-moment vectors by the corresponding component of vector (31), in accordance with definitions (20) and (21) we will get the average velocity and dispersivity of each species.

Whereas the completely general case that starts with an arbitrary initial condition $\vec{z}_o$ produces a fairly complicated analytical result for the mean velocities (see Appendix B), an interesting limit is one in which the perturbation is introduced in only one of the three species at a given time. For the special case of the initial condition $\vec{z}_o = [z_{o1}\ 0\ 0]^T$ (species

1 is only perturbed), the mean velocities of the three species turn out to be

$$\vec{u}^* = \begin{bmatrix} \dfrac{u_1k_2^2 + (2k_3u_1 + k_1u_2)k_2 + k_3(k_3u_1 + k_1u_3)}{(k_2 + k_3)(k_1 + k_2 + k_3)} \\ \dfrac{k_2u_1 + k_1u_2 + k_3(u_1 + u_2 - u_3)}{k_1 + k_2 + k_3} \\ \dfrac{k_3u_1 + k_1u_3 + k_2(u_1 - u_2 + u_3)}{k_1 + k_2 + k_3} \end{bmatrix}. \quad (33)$$

The dispersivities of the three species in this case are linear functions of time, independent of the initial perturbations, expressed by the following relation:

$$\frac{d}{dt}\vec{D}^* = \begin{bmatrix} \dfrac{k_1k_2k_3(u_2 - u_3)^2}{(k_2 + k_3)^2(k_1 + k_2 + k_3)} \\ \dfrac{k_3(u_1 - u_3)(u_3 - u_2)}{k_1 + k_2 + k_3} \\ \dfrac{k_2(u_1 - u_2)(u_2 - u_3)}{k_1 + k_2 + k_3} \end{bmatrix}. \quad (34)$$

Usually, when a particle diffuses, its mean-square displacement $\langle x^2(t)\rangle$ grows linearly in time. Deviations from this linear growth are known *anomalous diffusion* [$\langle x^2(t)\rangle \sim t^\alpha$; see [36,37]]. In our case, we have a fairly complicated non-Gaussian diffusion process in which the dispersivities are not only different but also linear functions of time. As a result the mean-square displacement grows faster than linearly in time ($\alpha=2$) and we have *super diffusion* (see [38]). If in addition the velocities of the unperturbed species are equal ($u_2=u_3$)—a typical example might be the situation in which the unperturbed binding species and the complex species are "immobilized," that is, $u_2=u_3=0$—the following relations hold:

$$u_1^* = u_2^* = u_3^* = \frac{(k_2 + k_3)u_1 + k_1u_2}{k_1 + k_2 + k_3}. \quad (35)$$

In this case the peak-to-peak separation distance between the centroids of species 1 and 3 is the same as 1 and 2 and expressed as

$$l_{1-2} = l_{1-3} = \frac{|u_2 - u_1|}{k_1 + k_2 + k_3} \quad (36)$$

and their dispersivities

$$\vec{D}^* = \begin{bmatrix} \dfrac{D_1(k_2 + k_3)^2(k_1 + k_2 + k_3)^2 + D_2k_1k_2(k_1 + k_2 + k_3)^2 + D_3k_1k_3(k_1 + k_2 + k_3)^2 + k_1(k_2 + k_3)^2(u_1 - u_2)^2}{(k_2 + k_3)(k_1 + k_2 + k_3)^3} \\ \dfrac{D_1(k_2 + k_3)(k_1 + k_2 + k_3)^2 + D_2(k_1 + k_3)(k_1 + k_2 + k_3)^2 - D_3k_3(k_1 + k_2 + k_3)^2 + k_1(k_2 + k_3)(u_1 - u_2)^2}{(k_1 + k_2 + k_3)^3} \\ \dfrac{D_1(k_2 + k_3)(k_1 + k_2 + k_3)^2 - D_2k_2(k_1 + k_2 + k_3)^2 + D_3(k_1 + k_2)(k_1 + k_2 + k_3)^2 + k_1(k_2 + k_3)(u_1 - u_2)^2}{(k_1 + k_2 + k_3)^3} \end{bmatrix}, \quad (37)$$

resulting in a convective-diffusion process in which the three species diffuse with their own respective dispersivities.

For the special case of the initial condition $\vec{z}_o = [z_{o1}\ z_{o1}\ z_{o3}]^T$ (binding species 1 and 2 are equally perturbed), the long-time mean velocities are independent of the initial concentrations and are expressed as follows:

$$\vec{u}^* = \begin{bmatrix} \dfrac{k_3u_1 + k_1u_3 + k_2(u_1 - u_2 + u_3)}{k_1 + k_2 + k_3} \\ \dfrac{k_3u_2 + k_2u_3 + k_1(-u_1 + u_2 + u_3)}{k_1 + k_2 + k_3} \\ \dfrac{u_3k_1^2 + (k_3u_1 + 2k_2u_3)k_1 + k_2(k_3u_2 + k_2u_3)}{(k_1 + k_2)(k_1 + k_2 + k_3)} \end{bmatrix}. \quad (38)$$

The dispersivities of the three species in this case is also a linear function of time, independent of the initial perturbations, expressed by the following relation:

$$\frac{d}{dt}\vec{D}^* = \begin{bmatrix} \dfrac{k_2(u_1 - u_2)(u_2 - u_3)}{k_1 + k_2 + k_3} \\ -\dfrac{k_1(u_1 - u_2)(u_1 - u_3)}{k_1 + k_2 + k_3} \\ \dfrac{k_1k_2k_3(u_1 - u_2)^2}{(k_1 + k_2)^2(k_1 + k_2 + k_3)} \end{bmatrix}. \quad (39)$$

Once again, we have a non-Gaussian diffusion process in which the dispersivities are no longer constant. If in addition the velocities of the binding species are also equal

$(u_1=u_2)$—a typical example might be the case of two identical binding species reacting via the following reaction $2A \rightleftharpoons C$, in which $k_1=k_2$—the following relations hold:

$$u_1^* = u_2^* = u_3^* = \frac{k_3 u_1 + (k_1 + k_2)u_3}{k_1 + k_2 + k_3}. \tag{40}$$

In this case the peak-to-peak separation distance between the centroids of species 1 and 3 is the same as 2 and 3 and expressed as

$$l_{1-3} = l_{2-3} = \frac{|u_3 - u_1|}{k_1 + k_2 + k_3} \tag{41}$$

and their dispersivities

$$\vec{D}^* = \begin{bmatrix} \dfrac{-D_2k_2(k_1+k_2+k_3)^2 + D_1(k_2+k_3)(k_1+k_2+k_3)^2 + (k_1+k_2)[D_3(k_1+k_2+k_3)^2 + k_3(u_1-u_3)^2]}{(k_1+k_2+k_3)^3} \\ \dfrac{-D_1k_1(k_1+k_2+k_3)^2 + D_2(k_1+k_3)(k_1+k_2+k_3)^2 + (k_1+k_2)[D_3(k_1+k_2+k_3)^2 + k_3(u_1-u_3)^2]}{(k_1+k_2+k_3)^3} \\ \dfrac{D_3(k_1+k_2)^2(k_1+k_2+k_3)^2 + k_3[D_1k_1(k_1+k_2+k_3)^2 + D_2k_2(k_1+k_2+k_3)^2 + (k_1+k_2)^2(u_1-u_3)^2]}{(k_1+k_2)(k_1+k_2+k_3)^3} \end{bmatrix}. \tag{42}$$

The velocities are again weighted averages of the individual advection velocities of the three species, with weighting coefficients that are related to the three rate constants k_i. In contrast with the binary case, in the ternary case the three species each disperse with their own separate effective dispersivities.

IV. DISCUSSION

Let us first discuss the binary case from a more intuitive physical (rather than mathematical) point of view. Consider what happens if an *equilibrium* mixture of two species C_1 and C_2 is injected as a plug into a CE device and driven through the capillary by application of an electric field. Provided that the mobilities of the two species are different, there is a tendency for the more mobile (faster) species to move ahead and the other to fall behind. This separation of the two species from the mixture, however, would perturb the reaction equilibrium and the reversible process in (22) would drive the locally C_1-rich and C_2-rich regions of the sample to undergo the appropriate forward or reverse reactions to restore that state of equilibrium. All the while, diffusion is also acting to spread the plug and smooth the concentration gradients. The competition between the advection trying to separate the species and the reaction trying to restore the equilibrium determines the overall concentration profiles that elutes from the CE. On average, the faster species turns out to be ahead of the slower species, but the two move at the same average speed. Meanwhile, the centroids in the two distributions attain a constant separation determined by the difference in the mobilities (velocities) and the reaction rates.

To see this more clearly, the solution to the coupled system of partial differential equations (11) has been obtained numerically using a finite-difference scheme and displayed in Fig. 1 in the form of the two concentrations as a function of space at various times. In discretizing this equation, we have used forward differencing for the temporal and central differencing for the spatial terms [39], allowing us to explicitly calculate the concentration of each species at each time interval. Also note that in generating the resulting graph, the equations were rendered dimensionless first using arbitrary scales so as to reproduce the starting equations with an identical although dimensionless set of parameters. The nondimensional values used in the simulation were $k_1=60$ and $k_2=40$ for the rate constants, $u_1=2$ and $u_2=1$ for the velocities, and $D_1=D_2=10^{-3}$ for the diffusivities of the two species.

As can be seen in Fig. 1, the equilibrium solution of the two species initially occupies a small region in space, with the two concentrations being uniform (and at equilibrium) within that region and zero outside. In time, the simulation shows that the two concentration profiles begin to separate and smooth out, resembling offset traveling Gaussians. As

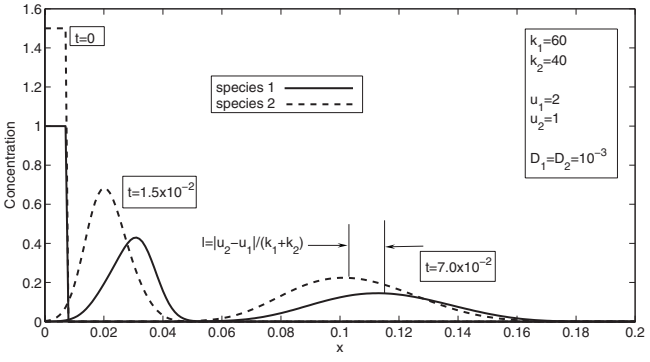

FIG. 1. Numerical simulation of the binary case showing the emergence of two approximate traveling Gaussians with fixed separation between the peaks.

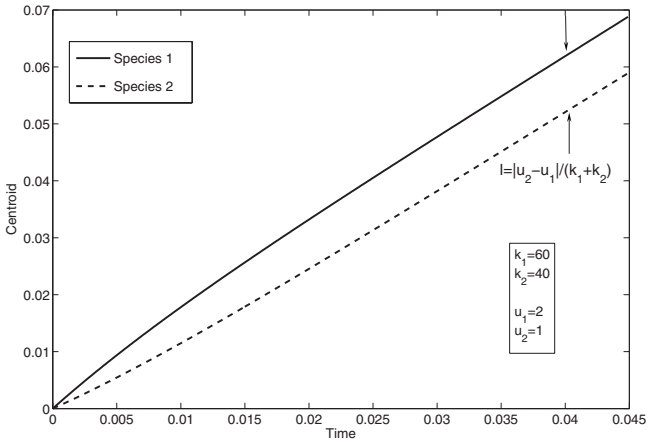

FIG. 2. The positions of the two centroids versus time obtained from the numerical solution.

time increases, further smearing (diffusion) of the profiles occurs although the peak-to-peak separation tends to a constant.

To verify that the centroids of the two distributions asymptotically translate at the same average speed and are offest by a constant, we have also computed the positions of the two centroids from the numerical data and plotted them as a function of time in Fig. 2. It can be seen that after an initial transient period [on the order of the reaction time, $1/(k_1+k_2)=10^{-2}$], the centroid curves do indeed achieve constant and equal slopes of 1.4, as given by Eq. (28), and the separation between the centroids tends to the constant 0.01, as given by Eq. (29).

It should also be noted that the overall long-time dispersivity of the binary mixture, as determined by Eq. (30) is 3.4×10^{-3} which is 3.4 times larger than the purely molecular diffusivity of the two species. In some cases, the contribution to the dispersivity arising from the difference in the electrophoretic mobilities and the reversible reaction rates might overwhelm the molecular contribution to the overall dispersion. Therefore, in experiments involving transport of chemically reactive species, one should recognize that the "band broadening" in the electropherogram might not be due to diffusivity alone.

For the binary case, the main results of our analysis are Eqs. (28)–(30) for the long-time mean velocity, asymptotic distance between the two centroids, and the mean dispersivity. The implication of these results is that, provided that the capillary is long enough so that during the time scale of the experiment, both the forward and reverse reactions can occur rapidly enough to establish a state of quasiequilibrium, the eluted concentration fields are approximately (and asymptotically) described by a pair of traveling Gaussians that travel at the same mean velocity, given by Eq. (28), but whose peaks are offset by the constant distance given by Eq. (29). In addition, the profiles diffuse axially with effective dispersion coefficient (30). We thus see the potential for extracting the kinetic rate constants k_1 and k_2 by measuring the mean velocity of the traveling profiles down the capillary and the peak-to-peak distance between the C_1-rich and C_2-rich parts of the field. Of course, the individual mobilities (i.e., migration velocities) of the two species must also be known (or measured) in advance.

In designing experiments to verify these theoretical results, the following important limitations should be born in mind. First, the time it takes for the species to traverse the length of the capillary, t_{expt}, needs to be long enough [i.e., long compared to the reaction times, $t_{expt}\gg(k_1+k_2)^{-1}$] for the long-time asymptotic limit discussed in this work to be reached. This implies the need for fairly fast reactions, at least compared to advection time scales. However, if the reaction rates are too high, the peak-to-peak separation (29) might be too small to be measurable. Also, the smearing distance due to dispersivity during the time of the experiment, $\sqrt{D^* t_{expt}}$, needs to remain small compared to the peak-to-peak separation to make the measurements practical.

The binary case described above represents the full behavior of a system in which a molecule can be in two different states and reversibly transform between those states with rate constants k_1 and k_2. It can also represent the full ternary binding system in the limit when the capillary is filled with one of the binding species at a concentration that is high compared to that of the second species. The second species is then injected locally into the capillary and its profile is observed while undergoing electrophoresis. In that case, the forward rate constant k_1 is itself a product of the association rate k_{on} and the initial uniform concentration of the more abundant species. Thus, one can envision repeating this experiment while varying the concentration of species that fills the capillary and examining the results as k_1 is thus varied, so as to determine the association and dissociation rates themselves. Our analysis therefore points out the potential for using standard ACE to measure both the rate and equilibrium constants of a binding reaction.

For the ternary case, the analytical results are more complicated and may be more difficult to apply in actual experiments. The limits that are easier to understand and work with are represented by Eqs. (33)–(42), which correspond to experiments in which the capillary is filled with an equilibrium mixture of all three binding species first, followed by introduction of a small local perturbation by the injecting only one of the species into the capillary and monitoring the subsequent electrophoresis. A particularly simple and interesting limit might be one in which one of the two binding species is "immobilized" (e.g., by covalently attaching it to a polymer network or hydrogel that fills the capillary) and only the other is mobile. In that limit, the velocities u_2 and u_3 are both zero (the complex also being immobile) and the only nonzero velocity component is therefore u_1. As such, when a perturbation from equilibrium is initially introduced in the mobile species concentration c_1, Eq. (33) suggests that the perturbation in the resulting centroids of all three concentrations propagate at the same speed, given by

$$u_1^* = u_2^* = u_3^* = \frac{(k_2+k_3)}{(k_1+k_2+k_3)}u_1, \tag{43}$$

and diffuse with the following dispersivities:

$$\vec{D}^* = \begin{bmatrix} \dfrac{D_1(k_2+k_3)^2(k_1+k_2+k_3)^2 + D_2k_1k_2(k_1+k_2+k_3)^2 + D_3k_1k_3(k_1+k_2+k_3)^2 + k_1(k_2+k_3)^2u_1^2}{(k_2+k_3)(k_1+k_2+k_3)^3} \\ \dfrac{D_1(k_2+k_3)(k_1+k_2+k_3)^2 + D_2(k_1+k_3)(k_1+k_2+k_3)^2 - D_3k_3(k_1+k_2+k_3)^2 + k_1(k_2+k_3)u_1^2}{(k_1+k_2+k_3)^3} \\ \dfrac{D_1(k_2+k_3)(k_1+k_2+k_3)^2 - D_2k_2(k_1+k_2+k_3)^2 + D_3(k_1+k_2)(k_1+k_2+k_3)^2 + k_1(k_2+k_3)u_1^2}{(k_1+k_2+k_3)^3} \end{bmatrix}. \quad (44)$$

Since the rate constants k_1 and k_2 are themselves related to the association rate constant k_{on} and the equilibrium concentrations of the two binding species in the prefilled capillary, as given by Eq. (16), one can again envision a series of dilution experiments in which the equilibrium concentrations in the prefilled capillary are varied, leading to variations in the observed mean velocity or elution time determined by Eq. (43). From such data, the original association and dissociation rate constants can thereby be determined.

One complicating factor that has not yet been considered in our analysis is the possibility of having "coupled" diffusion of the reacting species. In that case, the diffusivity matrix in the transport equations includes off-diagonal terms that represent the coupling. That is, gradients in the concentration of one of the species might induce diffusive fluxes in the others. Such issues have been considered in a different context by Leaist and co-workers [40–42].

Anomalous characteristics of dispersivities

In the ternary cases considered above, for certain choices of the parameters, it is possible to obtain dispersion coefficients that are negative for some of the species. For instance, it is evident from Eq. (37) or (44) that for large values of D_2 relative to D_1 and D_3, there is a possibility for negative dispersivity in species 3. At first sight, this is a surprising result since the dispersion coefficient is proportional to the time derivative of the mean-square displacement about the mean $\langle (x-\langle x\rangle)^2\rangle$ which, ordinarily, is a positive quantity that increases with time. However, the normal positivity of the mean-square displacement is based on the averaging operator $\langle\psi\rangle \equiv \int \psi c(x,t)dx / \int c(x,t)dx$, being defined using a nonnegative concentration field $c(x,t)$. In our case, the concentration fields used to define the moments represent small perturbations to the underlying equilibrium concentrations and, as such, are allowed to be of any sign. If a concentration perturbation is entirely negative, because it occurs in both the numerator and denominator of the averaging operator, the second central moment still turns out to be a positive growing quantity. However, when a perturbation concentration includes positive and negative regions, it is possible for the mean-square displacement about the mean to be negative. It should be noted that this anomalous characteristic of the dispersivity does not, by any means, imply band sharpening of the concentration field; rather, it is the result of the particular form of the perturbation in concentrations. To see this, we now consider a test case with negative dispersion and display the actual concentration field associated with it.

Consider the solution to the coupled system of partial differential equations (14) which has been obtained numerically using a finite-difference scheme similar to the binary case and displayed in Fig. 3 in the form of the three concentration perturbations as a function of space at a given time. The equations were rendered dimensionless first using arbitrary scales so as to reproduce the starting equations with an identical although dimensionless set of parameters. To simplify the analysis, the three species were assumed to be immobile (negative dispersion can occur even in the absence of advection) and an initial perturbation was introduced in species 1 only ($\tilde{c}_1=1$, $\tilde{c}_2=\tilde{c}_3=0$) of finite width centered about $x=0.5$. The nondimensional values used in the simulation were $k_1=k_2=k_3=1$ for the rate constants and $D_1=D_3=10^{-4}$ and $D_2=10^{-2}$ for the diffusivities of the three species.

In Fig. 3, the perturbation concentrations along the channel are plotted at time $t=3$. It is clear from the figure that species 1 remains positive throughout, whereas species 2 assumes an entirely negative profile and species 3 remains partially positive around the peak and negative about the two tails. However, the spatially averaged perturbation of species 3 is still positive as predicted by Eqs. (31) and (32). From a physical standpoint, we argue that initially due to excess amounts of C_1 in the center, there will be an enhanced binding reaction ($C_1+C_2 \rightarrow C_3$) at that location causing a depletion in C_2. This depletion gradually propagates outward (i.e., it causes C_2 to diffuse toward the central depleted region from the sides, reducing its concentration there), driving a dissociation reaction ($C_3 \rightarrow C_1+C_2$) in those regions and eventually leading to a depletion in C_3 about the two tails of the distribution.

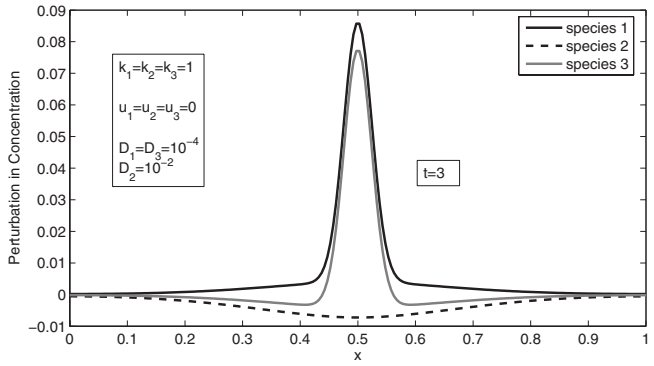

FIG. 3. Numerical simulation of the ternary case describing the anomalous characteristics of dispersivity seen in species 3.

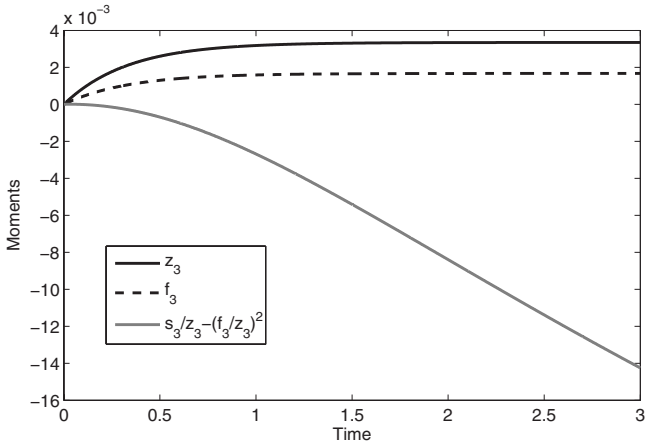

FIG. 4. Time evolution for various moments of species 3 obtained from the numerical simulation.

The resulting numerical data have been used to plot the various moments of species 3 as a function of time in Fig. 4. As seen in that figure, although the zeroth moment approaches a constant positive value, the second central moment $\langle (x-\langle x\rangle)^2\rangle$ becomes negative and decreases linearly in time. Indeed, since the concentration profile of species 3 is more spread out over its negative regions and is narrow and peaked around its positive regions (see Figure 3), a negative second central moment can be expected by examining the averaging operator. This negative second moment that decreases linearly in time yields a negative dispersivity for species 3, as predicted by the theory.

ACKNOWLEDGMENTS

This work was supported by the W. M. Keck Foundation and an NIH K25 grant (J.D.S.).

APPENDIX A: ANALYTICAL SOLUTION OF DIFFERENTIAL EQUATIONS

The systems of ordinary differential equations discussed in this paper can all be written in the general form

$$\frac{d\vec{y}}{dt} - K\vec{y} = \vec{a} + \vec{b}e^{\lambda_1 t} + \vec{c}te^{\lambda_1 t} + \vec{d}t, \tag{A1}$$

in which K is the matrix of reaction constants defined in Eq. (12) or (15) and λ_1 is the only nonzero eigenvalue of K. The vectors $\vec{a}$, $\vec{b}$, $\vec{c}$, and $\vec{d}$ are arbitrary constant vectors. First we investigate the homogenous problem ($\vec{a}=\vec{b}=\vec{c}=\vec{d}=\vec{0}$) whose solution is

$$\vec{y}(t) = e^{Kt}\vec{y}_0, \tag{A2}$$

where $\vec{y}_0$ is the initial condition. By denoting Λ as the diagonal matrix of eigenvalues of K and V as the matrix of right eigenvectors of K (so that $KV=V\Lambda$), it is understood that

$$e^{Kt} = Ve^{\Lambda t}V^{-1}. \tag{A3}$$

In the more general case ($\vec{a}\neq\vec{0}$, $\vec{b}\neq\vec{0}$, $\vec{c}\neq\vec{0}$, $\vec{d}\neq\vec{0}$), the solution is given by

$$\vec{y}(t) = e^{Kt}\vec{y}_0 + \int_0^t e^{K(t-\tau)}(\vec{a} + \vec{b}e^{\lambda_1\tau} + \vec{c}\tau e^{\lambda_1\tau} + \vec{d}\tau)d\tau. \tag{A4}$$

1. Ternary case

In the two cases discussed in this paper, the matrix K had the property of having one negative eigenvalue with all other eigenvalues being zero. Therefore the eigenvalue matrix Λ in general is of the form

$$\Lambda = \begin{bmatrix} \lambda_1 & 0 & 0 \\ 0 & 0 & 0 \\ 0 & 0 & 0 \end{bmatrix}, \tag{A5}$$

with $\lambda_1 < 0$. First we investigate the special case $\vec{a}=\vec{b}=\vec{0}$ for which we had $\vec{y}=e^{Kt}\vec{y}_0$, with $\vec{y}_0$ the initial condition. In order to compute e^{Kt}, we can first write its corresponding Taylor expansion in the form

$$e^{Kt} = I + \sum_{n=1}^{\infty} \frac{K^n t^n}{n!}. \tag{A6}$$

Substituting the corresponding eigendecomposition of K in this series yields

$$e^{Kt} = I + \sum_{n=1}^{\infty} \frac{(V\Lambda V^{-1})^n t^n}{n!} = V\left(I + \sum_{n=1}^{\infty} \frac{\Lambda^n t^n}{n!}\right)V^{-1},$$

resulting in

$$e^{Kt} = Ve^{\Lambda t}V^{-1}. \tag{A7}$$

At this stage, we make use of the fact that Λ has the special form (A5), and decompose $e^{\Lambda t}$ into two parts:

$$Ve^{\Lambda t}V^{-1} = V\left[I - \frac{(1-e^{\lambda_1 t})}{\lambda_1}\Lambda\right]V^{-1}, \tag{A8}$$

which ultimately simplifies e^{Kt} to

$$e^{Kt} = I - \frac{(1-e^{\lambda_1 t})}{\lambda_1}K. \tag{A9}$$

This approach reduces our calculations to a large extent and avoids the need for computing the eigenvectors of K.

Since we are interested in investigating the long-time behavior of the system (i.e., as $t\to\infty$ or, more physically, for times that are large compared to the reaction time $|\lambda_1|^{-1}$), let us define the matrix M as

$$M = \lim_{t\to\infty} e^{Kt} = I - \frac{K}{\lambda_1}. \tag{A10}$$

Matrix M has the special property that it is an oblique projection operator (K has a set of non-orthogonal eigenvectors)—that is,

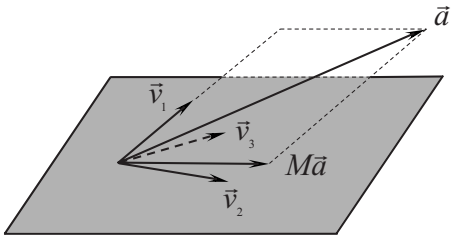

FIG. 5. Schematic representation of an arbitrary vector $\vec{a}$ being projected onto a plane containing $\vec{v}_2$ and $\vec{v}_3$ via the projection operator M.

$$M^2 = M. \tag{A11}$$

This can be seen intuitively because $\lim_{t\to\infty} e^{Kt} \sim \lim_{t\to\infty} e^{2Kt}$. This property could be better understood by expressing M in the following form:

$$M = I - \vec{v}_1 \vec{w}_1^T, \tag{A12}$$

where $\vec{v}_1$ and $\vec{w}_1$ are the right and left eigenvectors (covariant and contravariant base vectors) corresponding to the eigenvalue λ_1. These eigenvectors have the following relationship:

$$\vec{w}_i^T \vec{v}_j = \delta_{ij} \quad (i,j = 1,2,3). \tag{A13}$$

Also note that $\vec{w}_1^T$ can also be identified as the first row of V^{-1}, while $\vec{v}_1$ is the first column of V.

From a geometrical point of view, when operator (A12) is applied to an arbitrary vector, the latter is projected onto a plane containing $\vec{v}_2$ and $\vec{v}_3$ (eigenvectors corresponding to the zero eigenvalues) in such a way that its component in the $\vec{v}_1$ direction is removed. (When the projection operator is applied to the concentration vector, the concentration of the species approaches the *fixed plane* of the reaction in which they will reach a state of equilibrium.) Figure 5 illustrates this fact. This application of linear algebra is reminiscent of the seminal work of Wei and Prater [43], to quote from whose article, "The geometrical approach in terms of the kinetic problem, to linear algebra makes this branch of mathematics more appealing to the experimentalist. In fact, the ease with which the results and methods may be visualized in geometrical terms makes it a natural mathematics for the experimentalist."

For the particular case of the ternary system described by the rate constant matrix (15), the projection matrix M can be calculated and is given explicitly by

$$M = \frac{1}{k_1 + k_2 + k_3} \begin{bmatrix} k_2 + k_3 & -k_2 & k_3 \\ -k_1 & k_1 + k_3 & k_3 \\ k_1 & k_2 & k_1 + k_2 \end{bmatrix}. \tag{A14}$$

We now proceed to solve for $\vec{y}$ in the more general case ($\vec{a} \neq \vec{0}$, $\vec{b} \neq \vec{0}$, $\vec{c} \neq \vec{0}$, $\vec{d} \neq \vec{0}$). By substituting Eq. (A9) into Eq. (A4) and using the definition of M expressed in (A10), we get

$$\vec{y}(t) = e^{Kt}\vec{y}_0 + \int_0^t \left[M + \frac{e^{\lambda_1(t-\tau)}}{\lambda_1} K \right] (\vec{a} + \vec{b} e^{\lambda_1 \tau} + \vec{c}\tau e^{\lambda_1 \tau} + \vec{d}\tau) d\tau. \tag{A15}$$

Integrating this equation yields the following final result:

$$\vec{y}(t) = e^{Kt}\vec{y}_0 + A_1\vec{a} + A_2\vec{b} + A_3\vec{c} + A_4\vec{d}, \tag{A16}$$

where

$$A_1 = Mt + \frac{(e^{\lambda_1 t} - 1)}{\lambda_1^2} K, \tag{A17}$$

$$A_2 = \frac{(e^{\lambda_1 t} - 1)}{\lambda_1} M + \frac{t e^{\lambda_1 t}}{\lambda_1} K, \tag{A18}$$

$$A_3 = \frac{(\lambda_1 t e^{\lambda_1 t} - e^{\lambda_1 t} + 1)}{\lambda_1^2} M + \frac{t^2 e^{\lambda_1 t}}{2\lambda_1} K, \tag{A19}$$

$$A_4 = \frac{1}{2} M t^2 + \frac{(e^{\lambda_1 t} - 1 - \lambda_1 t)}{\lambda_1^3} K. \tag{A20}$$

2. Binary case

The matrix K in Eq. (12) is again singular, with eigenvalues $-(k_1+k_2)$ and 0 and with corresponding eigenvectors that are easy to obtain. The matrix of eigenvalues is thus given by

$$\Lambda = \begin{bmatrix} -(k_1 + k_2) & 0 \\ 0 & 0 \end{bmatrix}, \tag{A21}$$

and the corresponding matrix of eigenvectors is

$$V = \begin{bmatrix} -1 & k_2/k_1 \\ 1 & 1 \end{bmatrix}. \tag{A22}$$

The long-time solution of the homogeneous system will thus have the form

$$\lim_{t\to\infty} \vec{y}(t) = M\vec{y}_0, \tag{A23}$$

where matrix M now turns out to be

$$M = \frac{1}{k_1 + k_2} \begin{bmatrix} k_2 & k_2 \\ k_1 & k_1 \end{bmatrix}. \tag{A24}$$

For the nonhomogeneous problem, the results derived for the ternary case remain valid by simply substituting the corresponding 2×2 matrices M and K in Eqs. (A17)–(A19) and noting that the nonzero eigenvalue is given by $\lambda_1 = -(k_1+k_2)$.

APPENDIX B: LONG-TIME ANALYTICAL RESULTS FOR THE TERNARY CASE

Table II provides the long-time form of the effective velocities and the dispersivities of the three species in the ternary reaction case.

TABLE II. Long-time effective velocity and time derivative of diffusivity for the ternary reaction.

Effective velocity

$$\vec{u}^{*}=\begin{bmatrix}\dfrac{(z_{o1}-z_{o2})u_1k_2^2+\{k_1(z_{o1}-z_{o2})u_2+k_3[2z_{o1}u_1-z_{o2}(u_1+u_2-u_3)+z_{o3}(u_1-u_2+u_3)]\}k_2+k_3(z_{o1}+z_{o3})(k_3u_1+k_1u_3)}{(k_1+k_2+k_3)[k_2(z_{o1}-z_{o2})+k_3(z_{o1}+z_{o3})]}\\ \dfrac{(z_{o1}-z_{o2})u_2k_1^2+\{k_2(z_{o1}-z_{o2})u_1+k_3[-2z_{o2}u_2+z_{o3}(u_1-u_2-u_3)+z_{o1}(u_1+u_2-u_3)]\}k_1-k_3(z_{o2}+z_{o3})(k_3u_2+k_2u_3)}{(k_1+k_2+k_3)[k_1(z_{o1}-z_{o2})-k_3(z_{o2}+z_{o3})]}\\ \dfrac{(z_{o1}+z_{o3})u_3k_1^2+\{k_3(z_{o1}+z_{o3})u_1+k_2[2z_{o3}u_3+z_{o1}(u_1-u_2+u_3)+z_{o2}(-u_1+u_2+u_3)]\}k_1+k_2(z_{o2}+z_{o3})(k_3u_2+k_2u_3)}{(k_1+k_2+k_3)[k_1(z_{o1}+z_{o3})+k_2(z_{o2}+z_{o3})]}\end{bmatrix}$$

Time derivative of the effective diffusivity

$$\frac{d}{dt}\vec{D}^{*}=\begin{bmatrix}\dfrac{k_2k_3\{(z_{o1}+z_{o3})[k_3(z_{o2}+z_{o3})(u_1-u_2)+k_1(z_{o1}-z_{o2})(u_2-u_3)]+k_2(z_{o1}-z_{o2})(z_{o2}+z_{o3})(u_1-u_3)\}(u_2-u_3)}{(k_1+k_2+k_3)[k_2(z_{o1}-z_{o2})+k_3(z_{o1}+z_{o3})]^2}\\ -\dfrac{k_1k_3\{(z_{o1}+z_{o3})[k_3(z_{o2}+z_{o3})(u_1-u_2)+k_1(z_{o1}-z_{o2})(u_2-u_3)]+k_2(z_{o1}-z_{o2})(z_{o2}+z_{o3})(u_1-u_3)\}(u_1-u_3)}{(k_1+k_2+k_3)[k_1(z_{o1}-z_{o2})-k_3(z_{o2}+z_{o3})]^2}\\ \dfrac{k_1k_2(u_1-u_2)\{(z_{o1}+z_{o3})[k_3(z_{o2}+z_{o3})(u_1-u_2)+k_1(z_{o1}-z_{o2})(u_2-u_3)]+k_2(z_{o1}-z_{o2})(z_{o2}+z_{o3})(u_1-u_3)\}}{(k_1+k_2+k_3)[k_1(z_{o1}+z_{o3})+k_2(z_{o2}+z_{o3})]^2}\end{bmatrix}$$

[1] B. J. Sedlak, Genet. Eng. News **24**, 1 (2004).
[2] A. R. Kopf-Sill, Lab Chip **2**, 42 (2002).
[3] D. G. Myszka, Curr. Opin. Biotechnol. **8**, 50 (1997).
[4] P. Englebienne, A. V. Hoonacker, and M. Verhas, Spectroscopy **17**, 255 (2003).
[5] E. F. Fabrizio, A. Nadim, and J. D. Sterling, Anal. Chem. **75**, 5012 (2003).
[6] W. N. Vreeland, C. Desruisseaux, A. E. Karger, G. Drouin, G. W. Slater, and A. E. Barron, Anal. Chem. **73**, 1795 (2001).
[7] C. Galbusera and D. D. Y. Chen, Curr. Opin. Biotechnol. **14**, 126 (2003).
[8] Y. Tanaka and S. Terabe, Bol. Med. Hosp. Infant Mex **768**, 81 (2002).
[9] W. L. Tseng, H. T. Chang, S. M. Hsu, R. J. Chen, and S. M. Lin, Electrophoresis **23**, 836 (2002).
[10] N. H. H. Heegaard and R. T. Kennedy, Bol. Med. Hosp. Infant Mex **768**, 93 (2002).
[11] R. M. G. van Duijn, J. Frank, G. W. K. van Dedem, and E. Baltussen, Electrophoresis **21**, 3905 (2000).
[12] J. Y. Gao and P. L. D. B. B. Muhoberac, Anal. Chem. **69**, 2945 (1997).
[13] M. Berezovski and S. N. Krylov, J. Am. Chem. Soc. **124**, 13674 (2002).
[14] M. Berezovski, R. Nutiu, Y. F. Li, and S. N. Krylov, Anal. Chem. **75**, 1382 (2003).
[15] M. Berezovski, A. Drabovich, S. M. Krylova, M. Musheev, V. Okhonin, A. Petrov, and S. N. Krylov, J. Am. Chem. Soc. **127**, 3165 (2005).
[16] V. Okhonin, S. M. Krylova, and S. N. Krylov, Anal. Chem. **76**, 1507 (2004).
[17] G. I. Taylor, Proc. R. Soc. London, Ser. A **219**, 186 (1953).
[18] R. Aris, Proc. R. Soc. London, Ser. A **235**, 67 (1956).
[19] H. Brenner, PCH, PhysicoChem. Hydrodyn. **1**, 91 (1980).
[20] H. Brenner, PCH, PhysicoChem. Hydrodyn. **3**, 139 (1982).
[21] D. A. Edwards and H. Brenner, *Macrotransport Processes* (Butterworth-Heinemann, Stoneham, MA, 1993).
[22] B. J. Berne and R. Giniger, Biopolymers **12**, 1161 (1973).
[23] A. E. Degance and L. E. Johns, Chem. Eng. Sci. **30**, 1065 (1975).
[24] A. E. Degance and L. E. Johns, Appl. Sci. Res. **34**, 189 (1978).
[25] M. S. Bello, R. Rezzonico, and P. G. Righetti, Science **266**, 773 (1994).
[26] N. C. Stellwagen, S. Magnusdottir, C. Gelfi, and P. G. Righetti, Biopolymers **58**, 390 (2001).
[27] K. D. Dorfman and H. Brenner, Phys. Rev. E **65**, 021103 (2002).
[28] K. D. Dorfman and H. Brenner, Physica A **322**, 180 (2003).
[29] S. Ghosal and J. Horek, Anal. Chem. **77**, 5380 (2005).
[30] H. Poincaré, *Les Méthodes Nouvelles del la Mécanique Céleste* (Gauthier-Villars, Paris, 1892).
[31] A. M. Lyapunov, Ann. Math. Stat. **9**, 203 (1892).
[32] J. Hadamard, Bull. Soc. Math. France **29**, 224 (1901).
[33] V. A. Pliss, Izv. Akad. Nauk SSSR, Ser. Mat. **28**, 1297 (1964).
[34] A. Kelley, J. Differ. Equations **3**, 546 (1967).
[35] V. Balakotaiah and H. C. Chang, Philos. Trans. R. Soc. London, Ser. A **351**, 39 (1996).
[36] T. Geisel, J. Nierwetberg, and A. Zacherl, Phys. Rev. Lett. **54**, 616 (1985).
[37] M. Latini and A. J. Bernoff, J. Fluid Mech. **441**, 399 (2001).
[38] J. P. Bouchaud, A. Georges, J. Koplik, A. Provata, and S. Redner, Phys. Rev. Lett. **64**, 2503 (1990).

[39] J. C. Tannehill, D. A. Anderson, and R. H. Pletcher, *Computational Fluid Dynamics and Heat Transfer*, 2nd ed. (Taylor and Francis, Washington, DC, 1997).
[40] D. G. Leaist and N. Curtis, J. Solution Chem. **28**, 341 (1999).
[41] D. G. Leaist, Phys. Chem. Chem. Phys. **4**, 4732 (2002).
[42] K. MacEwan and D. G. Leaist, Phys. Chem. Chem. Phys. **5**, 3951 (2003).
[43] J. Wei and C. D. Prater, Adv. Catal. **13**, 203 (1962).